

Chapter 5: Nanoparticle Production from Cathode Sputtering in High-Pressure Microhollow Cathode and Arc Discharges

5.1. Introduction

Sputtering is a fundamental aspect of plasma operation and has been utilized to volatilize metal atoms for the purpose of manufacturing metallic interconnects, thin films, and patterned structures.[1-2] For many of these applications, the plasma is typically operated at low pressure with a well-defined sheath region above the cathode target. Positively charged ions are accelerated in this region, gaining sufficient translational energy[3] to induce sputtering when they strike the surface of the metal electrode. The ion energy gain in the sheath depends on the ion mean free path and, thus, the background neutral gas pressure. Numerous collisions at atmospheric pressure limit the ion energy gain and the ability to sputter the target material. Therefore, high-pressure plasmas are not very effective for sputtering.

Microhollow cathode (MHC) discharges[4] operating at atmospheric pressure have recently emerged as promising reactors for nanoparticle synthesis from gaseous precursors.[5][6] Since the cathode electrode confines the microdischarge, the ions are expected to sputter the cathode material. In this chapter, we demonstrate that cathode sputtering in the microdischarge produced extremely narrow size distributions of very small metal nanoparticles. We further compare the microdischarge sputtering results to those obtained from a high voltage arc discharge operated at atmospheric pressure at similar plasma power.

5.2. Experimental Method

The MHC discharge configuration[5] is shown in figure 5.1a. This is a short residence time reactor that permits the nucleation of particles but limits their growth as they are swept out of the small plasma volume. Rather than stainless steel electrodes that contain multiple elements, the setup consists of two oxygen-free high-conductivity (OFHC) copper electrodes, separated by a gap and enclosed in a glass tube and sealed with O-rings. The cathode is a single rod (O. D. \approx 38 mm) that has been machined to have a rodlike protrusion (O. D. \approx 4 mm) on one face through which a small hole (I. D. \approx 180 μ m) has been drilled on axis. This piece is biased negatively using a high-voltage DC power supply (Matsusada, Model AU-SR60) through a current limiting power resistor. The anode is a drilled (I. D. \approx 2 mm) OFHC copper piece, residing on a glass tube (O. D. \approx 3 mm) and connected to ground via a gold wire (O. D. \approx 130 μ m). The system is sealed on the anode side with an UltraTorr fitting, which helps align the glass tube with the hole in the cathode.

Argon flows through the cathode at 150 standard cubic centimeters per minute (sccm) and, upon exiting the cathode, is mixed with a second argon flow at 450 sccm to dilute the aerosol stream and limit agglomeration. The combined gas stream passes through the glass capillary and flows directly into the aerosol inlet of a nano-RDMA. This configuration allows particle size analysis *in situ* so that oxidation and other forms of contamination do not obfuscate particle size. The nano-RDMA instrument has been designed and calibrated to detect nanoparticles in the 1 nm size range.[7]

For comparison, an atmospheric pressure high-voltage arc discharge was constructed to interface with the nano-RDMA, as shown in figure 5.1b. Two OFHC

copper electrodes were inserted in a quartz cross (O. D. \approx 12.5 mm) and were sealed in place using O-rings. The cathode (grounded electrode) consisted of a flat surface while the anode (positively biased) was tapered to a point to reduce the electric field required to ignite the discharge. The arc was maintained with a high voltage power supply (Spellman X2094), connected to the electrodes in series with a current limiting power resistor (10 k Ω). The electrode gap spacing was fixed at 1 mm so that the voltage drop across the electrodes was approximately equal to the MHC discharge voltage drop. Comparisons between the two discharges were made at the same current and similar voltage drops across the plasma volume. A cross-flow of argon at 600 sccm was used to sweep the particles from the arc region into the nano-RDMA.

5.3. Results and Discussion

Both the microdischarge and the arc discharge produce neutral as well as charged nanoparticles of both charge polarities. The corresponding size distributions are presented in figures 5.2 and 5.3. These distributions are plotted in terms of absolute value of current measured with the faraday cup electrometer and the actual particle size and not in terms of mobility diameter.[8]

Fitting of the positively charged particle distributions with two log-normal distributions results in geometric mean mobility diameters of approximately 0.5 and 0.7 nm and geometric standard deviations of 1.1 and 1.2, respectively. The standard deviation value of the larger particle size is suggestive that the larger particle size is due to agglomeration of the smaller particles. Comparing the low and high current cases shown (and intermediate cases, not shown), the distributions remained similar in size, dispersity, and number concentration for a wide range of discharge currents (5 to 20 mA).

Consistent with the particle size regime, significantly fewer negatively charged particles were measured. Fitting of their distributions resulted in geometric means and geometric standard deviations identical to those for the positively charged particles produced at similar currents. Changes in the distributions and particle densities with discharge current were only slight. Unlike the positively charged particles, however, the second peak of the bimodal distribution was smaller than the first peak for all discharge currents. This observation may indicate that particle agglomeration occurs mainly in the discharge where charging dynamics can still influence particle polarity. In the absence of electric fields downstream from the microdischarge, we expect that the loss mechanisms are similar for both polarities.

It is important to note that these measured distributions represent a lower bound on particle concentration, as neutral particles are not counted. Furthermore, both charged and neutral particles may be lost to the walls by diffusion, electrophoresis, or thermophoresis, while in transit to the nano-RDMA. The exact concentration of particles produced in the microdischarge could not be measured.

The sputtered particles produced in the high-voltage arc discharge were different from those produced in the microdischarge, even when they both operate at atmospheric pressure and similar power and current. Interestingly, the particle size distributions for the arc discharge can be fit with a double lognormal distribution and the resulting geometric mean and geometric standard deviations are almost identical to the MHC discharge. Unlike in the MHC discharge distributions, however, the second peak grows significantly with current for both types of charged particles. While not shown, it was found that increasing the current beyond 30 mA produced particles significantly larger

than 1 nm and that the mean size continued to increase with current. The increase in particle size was attributed to a higher density of sputtered atoms produced in the arc discharge as the arc expands over the cathode surface. While not directly observable, a similar expansion in the plasma volume was believed not to occur in the microdischarge.

It was also observed that the arc produces a lower number of negatively charged particles than the microdischarge, although the positively charged particle numbers were similar for the two discharges operating under similar conditions. We speculate that this difference was indicative of the physical mechanism responsible for sustaining the microdischarge. As a result of the hollow cathode effect, the electrons in the microplasma were radially confined inside of the cathode where they undergo Pendel oscillations due to the radial electric field. The directional oscillation and a higher electron density due to confinement should increase the probability of electron attachment to clusters produced in the microdischarge. Alternatively, the larger number of negatively charged particles might indicate a lower neutral gas temperature in the MHC discharge as compared to the arc discharge. A higher gas temperature in the arc would increase thermionic emission of electrons from the particle, thereby reducing the fraction of the particles charged negatively. We have not attempted to measure neutral gas temperatures in these discharges.

Cathode sputtering in a microplasma is sufficiently generic that it should be applicable to different capillary materials. Though not shown in this section, high purity foils, fashioned into a capillary using a narrow diameter tungsten wire as a template, could be used for generic particle production. Sputtering was observed for gold, silver, platinum, zinc, palladium, vanadium, and molybdenum. Among all metals tried, a

significant increase in sputtered particle concentration was observed only for zinc with increasing discharge current.

5.4. Summary

Cathode sputtering in a microdischarge was shown to produce bimodal distributions of extremely small nanoparticles (diameters of ~ 0.5 and 0.7 nm). These distributions were distinct from those obtained using an atmospheric high-voltage arc discharge, with fewer negatively charged particles in the latter. Cathode sputtering in a microdischarge can be used for the production of generic nanoparticles by changing the cathode capillary.

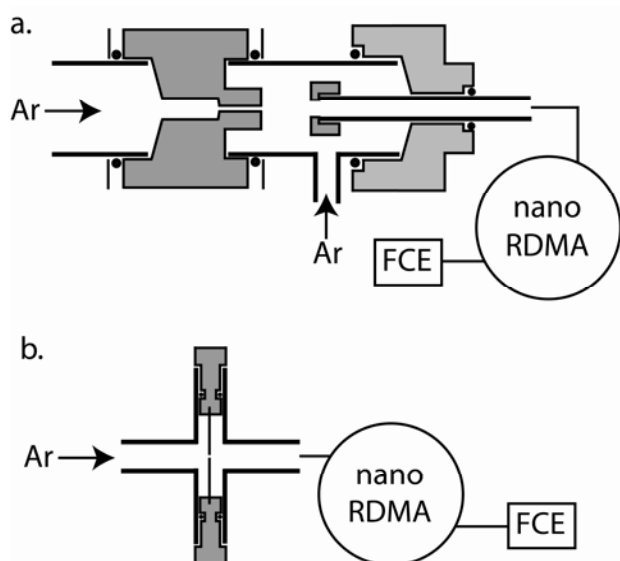


Figure 5.1. Schematic of Sputtering Discharges.

5.1a. Schematic of the MHC discharge and DMA set up used for *in situ* measurements of cathode sputtering. **5.1b.** Schematic of the arc discharge used for *in situ* measurements of sputtered particle size.

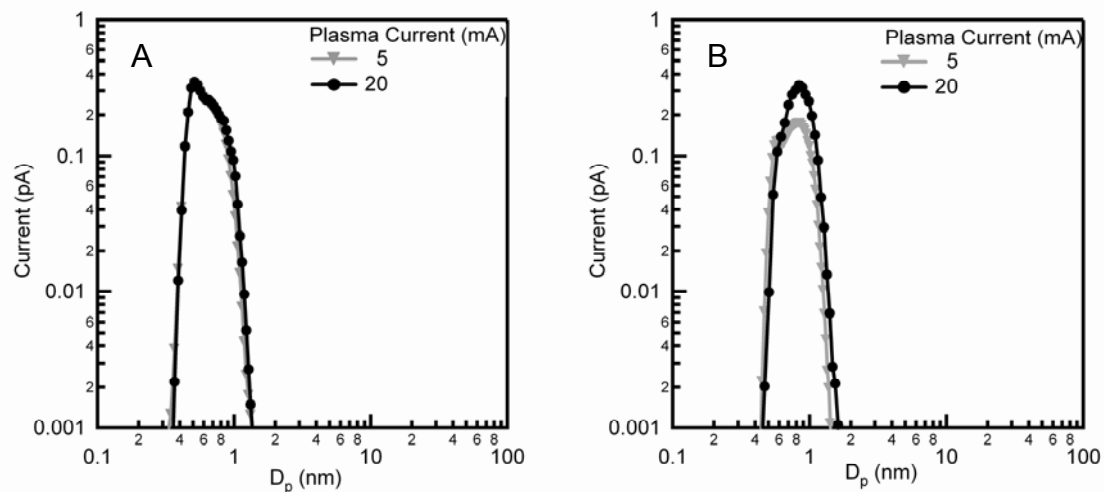


Figure 5.2. Size Distributions of Positively Charged Particles.

Size distributions of positively particles produced in (A) a microhollow cathode discharge (geometry 5.1a) and (B) an arc discharge (geometry 5.1b) operated at 1 atm in argon gas.

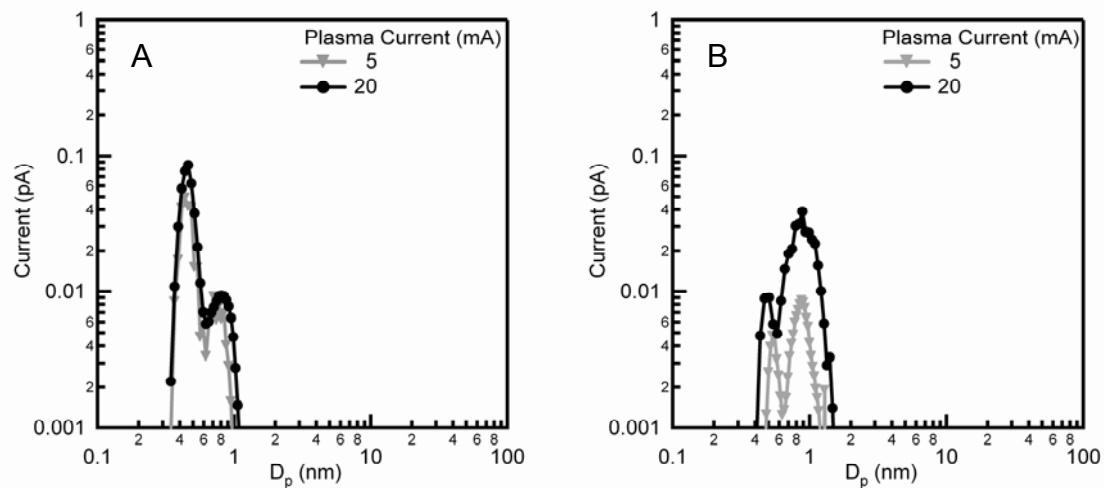


Figure 5.3. Distribution of Negative Charged Particles.

Size distributions of negatively charged particles produced in (A) a microhollow cathode discharge and (B) a high-voltage arc discharge operated at 1 atm in argon.

References

1. S. Rossnagel, and J. Hopwood, *Journal of Vacuum Science & Technology B: Microelectronics and Nanometer Structures*, **12**, 449, 1994.
2. J. J. Cole, E.-C. Lin, C. R. Barry, and H. O. Jacobs, *Applied Physics Letters*, **95**, 113101, 2009.
3. M. A. Lieberman, and A. J. Lichtenberg, *Principles of Plasma Discharges and Materials Processing*. (Wiley-Interscience, Hoboken, NJ, ed. Second, 2005).
4. R. M. Sankaran, and K. P. Giapis, *Journal of Applied Physics*, **92**, 2406, 2002.
5. R. Sankaran, D. Holunga, R. Flagan, and K. Giapis, *Nano Letters*, **5**, 537, 2005.
6. K. Becker, K. Schoenbach, and J. Eden, *Journal of Physics-London-D Applied Physics*, **39**, 55, 2006.
7. N. Brunelli, R. Flagan, and K. Giapis, *Aerosol Science and Technology*, **43**, 53, 2008.
8. H. Tammet, *Journal of Aerosol Science*, **26**, 459, 1995.